Gas Generation Model for OPG's Low and Intermediate Level Radioactive Waste Deep Geologic Repository

K. Sedor[1], P. Suckling[2], P. Humphreys[3], F. King[4]
[1] Nuclear Waste Management Organization, Toronto, Ontario, Canada
[2] Quintessa Ltd., Henley-on-Thames, Oxfordshire, United Kingdom
[3] University of Huddersfield, Queensgate, Huddersfield, United Kingdom
[4] Integrity Corrosion Consulting Ltd., Nanaimo, British Columbia, Canada

Abstract

As part of the postclosure safety assessment for Ontario Power Generation's (OPG) Deep Geologic Repository (DGR) for low and intermediate level waste (L&ILW), gas generation modelling has been undertaken. A variety of microbial and corrosion processes were considered for the generation of gases and the consumption of water within the repository. Four key mechanisms have been identified: microbial degradation of organic waste, methanogenesis, corrosion of metallic wastes, and CO_2 enhanced corrosion of metallic wastes.

1. Introduction

Ontario Power Generation (OPG) is proposing to build a Deep Geologic Repository (DGR) for Low and Intermediate Level Waste (L&ILW) near the existing Western Waste Management Facility (WWMF) at the Bruce nuclear site in the Municipality of Kincardine, Ontario (Figure 1). The repository will be located approximately 680 m below surface within very low permeability limestones, overlain by about 200 m of very low permeability shales. The Nuclear Waste Management Organization, on behalf of OPG, is currently preparing an Environmental Impact Statement (EIS) and Preliminary Safety Report (PSR) for the proposed repository.

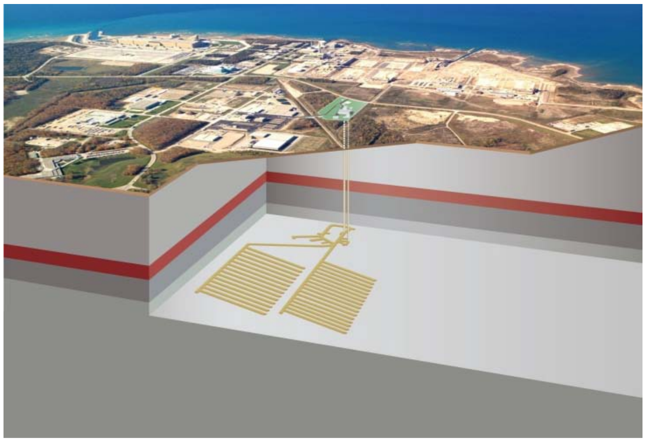

Figure 1: The DGR Concept at the Bruce Nuclear Site

The safety assessment (SA) of the proposed facility considers the generation of gases in the repository and migration of those gases through the geosphere. To carry out this task, a gas generation model coupled with a two-phase flow transport code has been developed, called T2GGM. The gas generation model (GGM) calculates the gas generation and water consumption rates based on the microbial and corrosion processes occurring in the repository and the environmental conditions, such as pressure, saturation and relative humidity. TOUGH2 (T2) is a two-phase flow transport code, which tracks the migration of gases away from the repository. T2GGM allows for a detailed representation of the repository and geosphere.

The focus of the current paper is the GGM. The generation of gases from the degradation of organic waste by microbial processes and the corrosion of metallic waste and container materials will be discussed, and the key gas generation processes will be identified. The gas modelling work presented here is described in full in technical report [1]. It forms part of a suite of related SA studies summarised in the interim (V1) Postclosure SA report [2]. A technical paper on T2GGM, the coupled gas generation and two-phase flow transport code, has been presented elsewhere [3].

2. Microbial gas generation reactions

2.1 Degradation of organics

Organic wastes to be emplaced in the DGR are categorized as: cellulose, ion-exchange resins, and plastics and rubbers. These wastes typically consist of long-chain polymers, which are degraded by a complex multistage process involving a large array of microbial species [4,5]. The microbial degradation of cellulose is well documented [5,6], where as the degradation of resins, plastics and rubbers is less well established [6].

Initially, the large polymers are broken down into smaller, pieces. The intermediates can be oxidized by a range of terminal electron acceptors (TEAs) employed by microbial systems. These TEAs are consumed in a well-defined order depending on the amount of energy provided by each reaction: oxygen, nitrate, ferric ion, manganese, sulphate, and carbon dioxide.

For modelling purposes, the degradation of organics can be simplified by the fact that the conversion of polymeric substrates to their intermediates (for example, the separation of cellulose into glucose monomers) is often the rate limiting step in the gas generation process [7]. This allows the microbial oxidation of polymeric substrates to be coupled directly to the reduction of the relevant TEA. The degradation of polymeric substrates then becomes a single-stage process with the consumption of TEAs being instantaneous and controlled by the rate of polymer degradation. Conservatively, this approach assumes that the degradation of organics proceeds to completion (i.e. to gas), with no accumulation of intermediate products. As well, the model assumes that all microbial groups required to catalyze the process modelled are present within the repository.

2.1.1 Cellulose

Cellulose is a polymer of anhydroglucose which is broken down to glucose monomers via hydrolysis:

$$(C_6H_{10}O_5)_n + n\ H_2O \rightarrow n\ C_6H_{12}O_6 \qquad (1)$$

However, the generation of glucose intermediates is avoided by coupling the oxidation of cellulose directly to the reduction of TEAs using the approach outlined in Section 2.1. The oxidation of cellulose by oxygen, nitrate, ferric ion, sulphate and carbon dioxide are modelled by the following reactions, respectively:

$$C_6H_{10}O_5 + 6O_2 \rightarrow 6CO_2 + 5H_2O \tag{2}$$

$$5C_6H_{10}O_5 + 24NO_3^- + 24H^+ \rightarrow 30CO_2 + 12N_2 + 37H_2O \tag{3}$$

$$C_6H_{10}O_5 + 24Fe(III) + 7H_2O \rightarrow 6CO_2 + 24Fe(II) + 24H^+ \tag{4}$$

$$C_6H_{10}O_5 + 3SO_4^{2-} + 6H^+ \rightarrow 6CO_2 + 5H_2O + 3H_2S \tag{5}$$

$$C_6H_{10}O_5 + H_2O \rightarrow 3CO_2 + 3CH_4 \tag{6}$$

where the reaction rate for all these is that for cellulose hydrolysis, Equation (1), with different rates of hydrolysis under aerobic (Reactions (2) and (3)) and anaerobic conditions (Reactions (4), (5), and (6)).

2.1.2 Ion-exchange resins

Ion-exchange resins consist of a polystyrene divinyl benzene backbone. Cation exchange resins are acidic, with sulphonic acid functional groups, and anion exchange resins are basic, with quaternary amine functional groups. The functional groups on the resins are an appreciable fraction of the resin mass, but do not contain carbon, and so do not contribute to the gas generation. The polystyrene divinyl benzene backbone is broken down to soluble intermediates according to Figure 2.

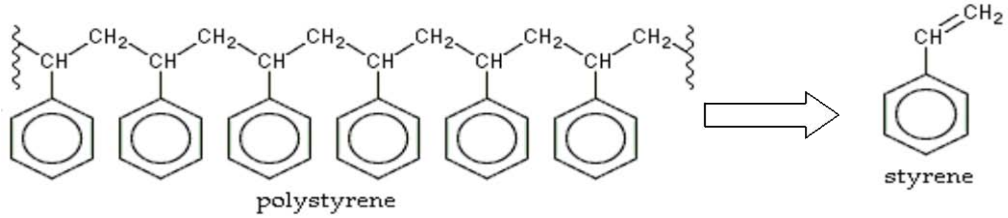

Figure 2: Polystyrene hydrolysis

The oxidation of styrene monomer by oxygen, nitrate, ferric ion, and sulphate and methanogenesis are modelled by the following reactions, respectively:

$$C_8H_8 + 10O_2 \rightarrow 8CO_2 + 4H_2O \tag{7}$$

$$C_8H_8 + 8NO_3^- + 8H^+ \rightarrow 8CO_2 + 4N_2 + 8H_2O \tag{8}$$

$$C_8H_8 + 40Fe(III) + 16H_2O \rightarrow 8CO_2 + 40Fe(II) + 40H^+ \tag{9}$$

$$C_8H_8 + 5SO_4^{2-} + 10H^+ \rightarrow 8CO_2 + 4H_2O + 5H_2S \tag{10}$$

$$C_8H_8 + 6H_2O \rightarrow 3CO_2 +5CH_4 \tag{11}$$

where the reaction rates for all these are that for polystyrene degradation, Figure 2, again using different rates for aerobic and anaerobic processes.

2.1.3 Plastics and Rubbers

The plastic and rubber components of radioactive waste include a mix of materials such as PVC, polyethylene, neoprene, nitrile, and latex. The heterogeneous nature of this waste category makes it difficult to model in detail since the degradation of each material would have to be modelled explicitly with an individual inventory and reaction scheme for each component. In order to assess the potential impact of plastic and rubber degradation on the overall gas generation in the repository these components are modelled as having a resin-like C_8H_8 organic composition, but with a unique degradation rate. This maximizes the amount of carbon and therefore the potential gas generated, and provides the appropriate timescale for their degradation, without the need for detailed degradation pathways for each component.

2.2 Microbial hydrogen mechanism

There are a large number of microbial processes able to process hydrogen [5,7]. In the DGR, a significant amount of hydrogen will be produced from corrosion of metallic waste. In the Postclosure Safety Assessment (V1) Report [2], three hydrogen mechanisms were considered: the oxidation of hydrogen by ferric ion and sulphate reduction, and methanogenesis.

2.2.1 Ferric ion and sulphate hydrogen mechanisms

Ferric ion and sulphate metabolize hydrogen in the saturated phase. Ferric ion is a soluble intermediate in the corrosion process (as shown in Section 3). Sulphate will be initially present in waste emplaced in the DGR, and will continue to enter the repository by seeping in from the surrounding rocks. These two electron acceptors will oxidize hydrogen by iron reduction and sulphate reduction, respectively:

$$H_2 + 2Fe(III) \rightarrow 2Fe(II) + 2H^+ \tag{12}$$

$$4H_2 + SO_4^{2-} + 2H^+ \rightarrow H_2S + 4H_2O \tag{13}$$

Both ferric ion and sulphate reduction will only occur in the saturated region. The repository is expected to remain largely unsaturated for tens of thousands of years or longer [2], and so these are not dominant hydrogen oxidation mechanisms.

2.2.2 Methanogenesis

Methanogens present in the closed repository will turn the available hydrogen and carbon dioxide into methane according to the methanogenic reaction:

$$CO_2 + 4H_2 \rightarrow CH_4 + 2H_2O \tag{14}$$

The activity of methanogens is an important factor in the generation and build-up of gases in the repository. The methanogenic reaction decreases the number of gas moles by 4 (since 4 moles of hydrogen and 1 mole of carbon dioxide are required to create 1 mole of methane), and as a result, decreases the pressure in the DGR.

Methanogens are ubiquitous in environments where oxygen is absent [4]. The methanogenic reaction can occur in saturated and unsaturated conditions as long as there is sufficient humidity to support microbial processes. These bacteria flourish in strict anaerobic environments where sulphate, oxidized metals and nitrate are absent [8]. The DGR will meet these requirements several decades after closure, at which point the first 4 stages of TEAs (oxygen, nitrate, ferric ion, and sulphate reduction) will be complete. Very small amounts of TEAs seeping in from surrounding rock will be confined to the saturated region where they will be reduced. When active, methanogens can rapidly consume hydrogen [8,9].

2.3 Biomass generation, decay and recycling

The microbial biomass present in the DGR was also considered in the GGM. Significant amounts of water may be held up in microbial biomass (as these cells are typically 80% w/w water). Consequently, there must be sufficient water to complete the oxidation-reduction reactions and to support the production of microbial cells. The availability of water may be rate limiting under low-permeability environments such as the DGR [10].

The reactions representing biomass generation from cellulose, styrene and hydrogen, respectively, are represented by

$$5C_6H_{10}O_5 + 6NH_3 + 137H_2O \rightarrow 6C_5H_7O_2N\cdot 25H_2O \quad (15)$$

$$C_8H_8 + 2NH_3 + 2CO_2 + 50H_2O \rightarrow 2C_5H_7O_2N\cdot 25H_2O \quad (16)$$

$$5CO_2 + 10H_2 + NH_3 + 17H_2O \rightarrow C_5H_7O_2N\cdot 25H_2O \quad (17)$$

Cellulose and styrene degradation will involve both TEA reduction (as discussed in Sections 2.1.1 and 2.1.2, respectively) and biomass production. For modelling purposes, a biomass yield factor is used to represent the division of cellulose and styrene between biomass production and degradation products. It is conservatively assumed that ammonia is always available.

Microbial biomass is subject to natural turnover since cells have finite lifetimes. Biomass contains a range of compounds, which have different degradabilities. Some microbial cell components are recalcitrant to further degradation and accumulate in the environment. In the present model both easily recyclable and recalcitrant biomass are considered. Easily recyclable biomass is modelled as being converted first back to cellulose via

$$6C_5H_7O_2N\cdot 25H_2O \rightarrow 5C_6H_{10}O_5 + 6NH_3 + 137H_2O \quad (18)$$

Recalcitrant biomass is assumed to lose its water but otherwise undertake no further reactions.

3. Corrosion of metallic waste and container materials

Metallic materials to be emplaced in the DGR are classified as: carbon and galvanized steels, passivated carbon steels, stainless steels and nickel alloys, and zirconium alloys.

The corrosion of carbon and galvanized steel are treated as one, neglecting the thin zinc coating on galvanized steel. For simplicity, the corrosion of carbon and galvanized steel is represented by the corrosion of the dominant metal element, Fe. Passivated carbon steels are waste forms grouted in cementitious materials and structural steel in contact with concrete. They are also modelled using the corrosion of Fe, but with a slower reaction rate compared to that of carbon steel due to the effects of the alkaline concrete pore water. The corrosion rate of stainless steel and nickel alloys is slower than for carbon and galvanized steel because of the formation of a (Cr-rich) passive film. For simplicity, the corrosion of these alloys is treated in the same manner as for carbon steel, but at a slower rate. The corrosion of zirconium alloy is represented by the oxidation of zirconium (Zr) [1].

Corrosion of metallic waste is considered for a variety of repository conditions. Aerobic conditions will exist in the repository shortly after closure. Oxygen will act as an oxidant for the corrosion process, but will quickly be depleted. In anaerobic conditions, water will replace oxygen as an oxidant. The repository will also be partially saturated after closure with water originating from the host rock. Corrosion can occur in saturated or humid conditions.

3.1 Aerobic

Under aerobic conditions, metallic waste is oxidized according to the reaction:

$$4Fe + 2H_2O + 3O_2 \rightarrow 4\ \text{“FeOOH”} \qquad (19)$$

where “FeOOH” represents an un-specified ferric oxyhydroxide species, which may also contain groundwater species (Cl^-, SO_4^{2-}, CO_3^{2-}) in various forms of green rust.

As anaerobic conditions develop, the Fe(III) corrosion product (resulting from the aerobic corrosion of steel) is converted to Fe(II) via

$$2FeOOH + Fe + 2H_2O \rightarrow 3Fe(OH)_2 \qquad (20)$$

3.2 Anaerobic

Under anaerobic conditions, the metallic waste is oxidized by H_2O:

$$Fe + 2H_2O \rightarrow Fe(OH)_2 + H_2 \qquad (21)$$

Ferrous hydroxide may be converted to magnetite via the Schikkor reaction, leading to the formation of magnetite, water and additional hydrogen.

$$3Fe(OH)_2 \rightarrow Fe_3O_4 + 2H_2O + H_2 \qquad (22)$$

Anaerobic corrosion of steel in the DGR is represented by the overall reaction (a combination of equations 21 and 22):

$$3Fe + 4H_2O \rightarrow Fe_3O_4 + 4H_2 \qquad (23)$$

The anaerobic corrosion of zirconium alloys is given by the following reaction:

$$Zr + 2H_2O \rightarrow ZrO_2 + 2H_2 \qquad (24)$$

3.3 CO_2 enhanced corrosion

High partial pressures of carbon dioxide, produced by the degradation of organic waste, will accelerate the rate of corrosion for carbon and galvanized steel, and stainless steel and nickel alloys. Pure, dry carbon dioxide is not corrosive. However, when dissolved in water, carbon dioxide forms carbonic acid (H_2CO_3) which is corrosive.

$$CO_2 + H_2O \leftrightarrow H_2CO_3 \qquad (25)$$

The enhancement of corrosion by carbon dioxide can be described by:

$$Fe + CO_2 + H_2O \rightarrow FeCO_3 + H_2 \qquad (26)$$

The factors that will affect the corrosion rate include the partial pressure of carbon dioxide, temperature, and acidity. In the Postclosure SA Report [2], the enhancement of steel corrosion by carbon dioxide is represented by a simple enhancement factor (F):

$$F = 1 + \left(\frac{P_{CO_2}}{P_{CO_2}^{ref}}\right)^q \tag{27}$$

where P_{CO2}^{ref} is a reference carbon dioxide partial pressure at which the corrosion rate is twice that in the absence of carbon dioxide and q is the reaction order with respect to the partial pressure of carbon dioxide. The value for q of 0.67 is based on the reaction order reported by deWaard and Milliams [11]. The corrosion rate expression proposed by these authors cannot be used directly to estimate a value of P_{CO2}^{ref} since the expression is undefined in CO_2-free solution. Instead, a corrosion rate for CO_2-free conditions, but under the same high rates of mass transport as considered by deWaard and Milliams, was estimated from the literature. The original deWaard and Milliams expression was then used to predict the P_{CO2} at which this rate would be doubled due to the presence of CO_2.

4. Water limitation and humidity

The DGR is situated in tight rock from which groundwater will slowly seep into the repository. As organic degradation, microbial hydrogen consumption and corrosion proceed, gas pressures will increase and water will be consumed. This may cause the saturation to drop to very low levels, which can be accompanied by a drop in relative humidity. The GGM takes into account water limitation and changes in humidity.

Once the water saturation in the DGR has reached zero, the water-consuming microbial and corrosion reactions become water limited. GGM then calculates the rate at which these reactions proceed based on the water supply rate. The vapour phase microbial and corrosion processes in the DGR are dependent on relative humidity. This is modelled by a smooth reduction in reaction rates as humidity decreases from 80% to 60%, ceasing when the lower limit is reached.

5. GGM Output

The GGM is capable of running coupled with TOUGH2 or standalone. When coupled to TOUGH2, values defining the geosphere response are passed to the GGM at each time step: the repository void volume, average gas pressure, total water saturation, and average relative humidity. When running GGM standalone, a driver program using a simple geosphere model replaces TOUGH2 to provide an approximate geosphere response. The parameters for the simple model employed by the driver program are chosen by roughly fitting the results from a reference T2GGM simulation.

The results obtained when running the standalone GGM are not for the purpose of modelling the DGR, but rather for the purpose of testing the GGM and determining the key reactions (the reactions that generate/consume large quantities of gas, influencing the overall pressure profile in the DGR, and those which do not). As well, the standalone GGM can determine dominant gas in the repository over long time-scales. These key factors can be identified using the standalone GGM, and applied to the more detailed, integrated modelling. The advantage of the standalone GGM over T2GGM is a reduction of run time.

The results from GGM standalone are presented in the following sections. This case incorporates all functions of the GGM, as discussed in Section 2 to 4.

5.1 Terminal electron acceptor stages

Figure 3 shows the terminal electron acceptor stages. These are: (1) aerobic degradation, (2) nitrate reduction, (3) ferric ion reduction, (4) sulphate reduction, and (5) methanogenesis. The initial four stages complete within approximately 10 years after repository closure.

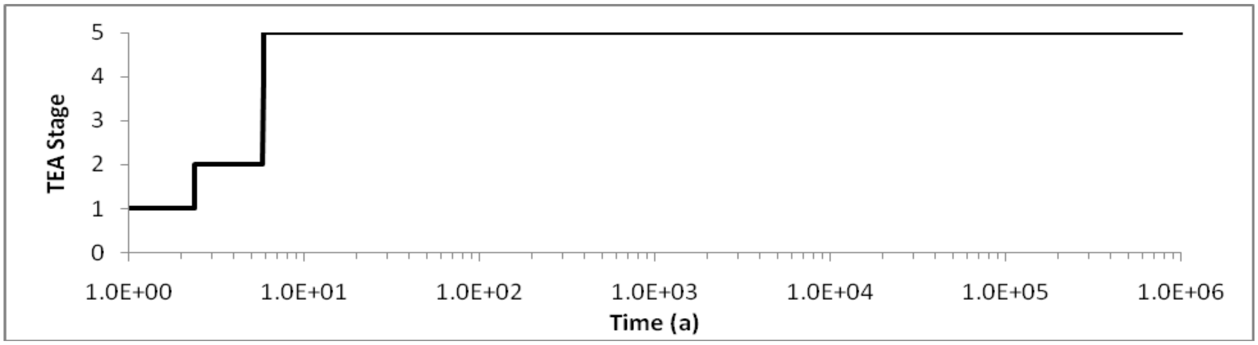

Figure 3: Terminal Electron Acceptor Stages

5.2 Gas generation

The calculated gas partial and total pressures within the repository are given in Figure 4. The total gas pressure reaches a peak pressure of 8.4 MPa at approximately 20,000 years. This is slightly higher than the steady-state pressure in the geosphere at repository depth of approximately 7.6 MPa.

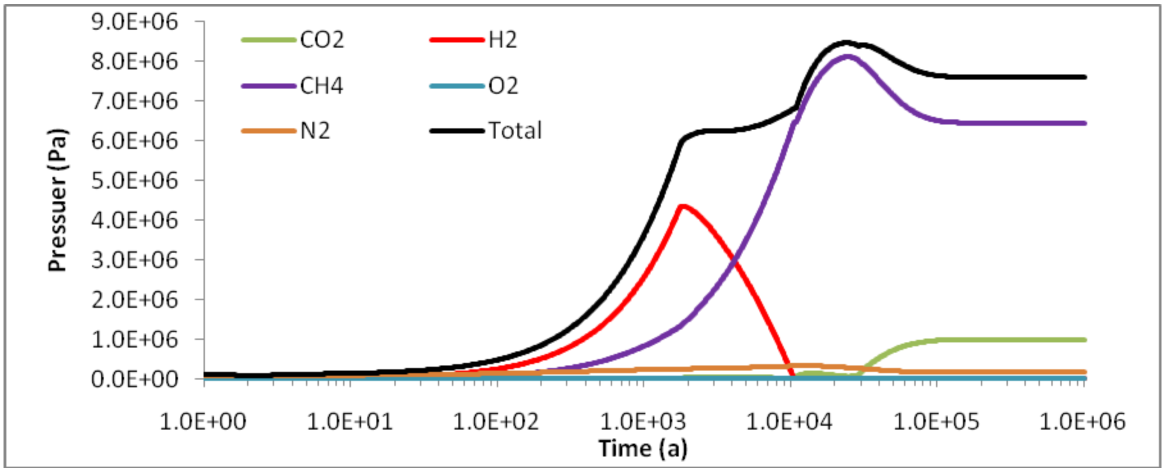

Figure 4: Total and partial gas pressures within the repository

Methane is the dominant gas within the repository, produced by both the microbial degradation of organic wastes and by the methanogenic reaction. Most of the carbon initially in the organic waste streams is ultimately converted to methane gas within 100,000 years.

Carbon dioxide is produced by the degradation of organic wastes in the repository and consumed by the methanogenic reaction, enhanced corrosion of steel and the production of biomass. Throughout the evolution of the repository, carbon dioxide is maintained at low partial pressures.

Hydrogen is produced by the corrosion of metallic wastes in the repository. Consumption of hydrogen gas occurs rapidly by the methanogenic reaction, as well as biomass growth. Hydrogen is completely consumed at approximately 10,000 years.

Oxygen is depleted quickly in the DGR. Anaerobic conditions are established in 2 years after repository closure. Nitrogen is present in the DGR upon closure. Additional nitrogen is produced during the nitrate reduction TEA stage, which is complete at approximately 10 years after repository closure. Nitrogen is not consumed, as it does not play a role in the microbial or corrosion reactions considered in the model.

Trace levels of hydrogen sulphide are produced during the sulphate reduction stage. The amount produced is insufficient to appear on the plot, and rapidly precipitates as iron sulphide.

5.3 Organic wastes

The degradation of the organic wastes is shown in Figure 5. Complete degradation of all of the waste streams is calculated to occur at around $4x10^5$ years. Recycling of dead biomass as cellulose-like organic material is responsible for delaying the time at which the cellulose is completely consumed. Without biomass recycling, this waste stream would have been completely consumed at approximately $4x10^4$ years.

The calculated amounts of live biomass and the total amount of dead (recalcitrant) biomass are shown in Figure 6. The growth of methanogens can be limited by the availability of H_2 and CO_2. At approximately $8x10^3$ years hydrogen gas within the repository is completely consumed (as shown in Figure 4). From this point forward, the methanogenic biomass production is limited by the rate at which hydrogen is produced through corrosion. Once the corrosion of metallic waste is complete, and no more hydrogen is produced, the growth of biomass ceases. The remaining methanogens die, and some are recycled to cellulose with recalcitrant biomass remaining. Only a small fraction (4%) of the carbon atoms in the system (originally in the form of organic waste) end up as recalcitrant biomass. It is assumed that 10% of biomass is recalcitrant [1].

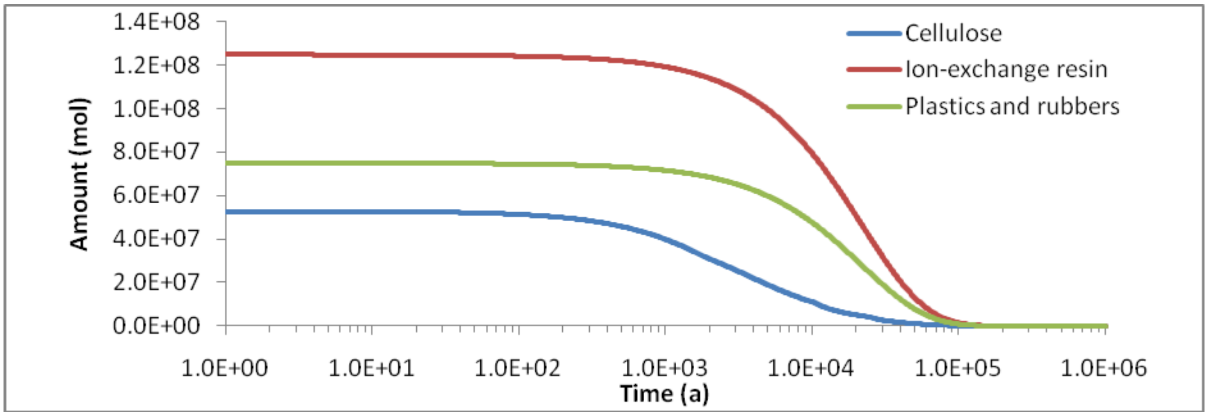

Figure 5: Amount of Organic Waste

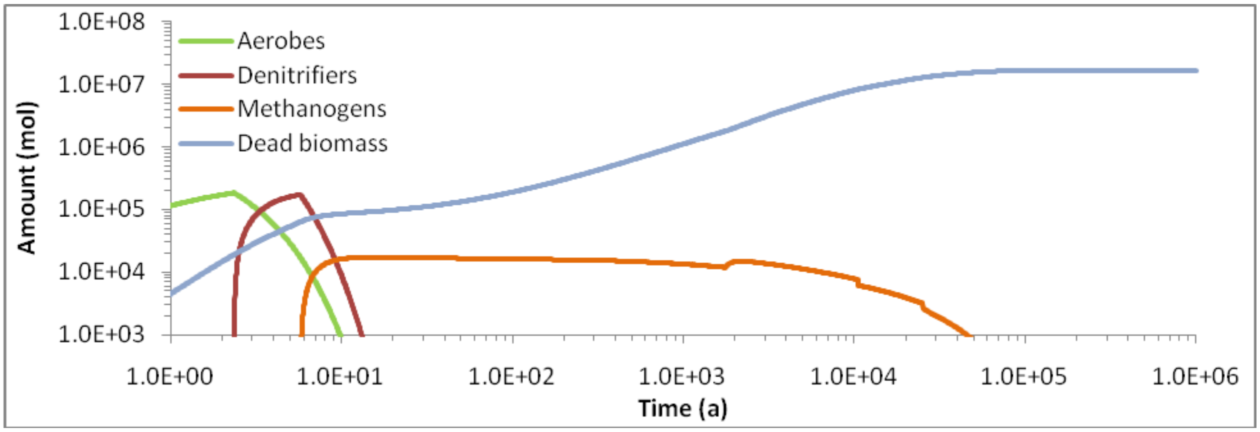

Figure 6: Amounts of live and total dead (recalcitrant) biomass

5.4 Metallic wastes

The different types of metallic wastes are consumed at various times. Carbon and galvanized steels, passivated carbon steels, stainless steel and nickel based alloys, and zirconium alloys are calculated to be consumed at 2x10^3, 10^5, 3x10^4, and 3x10^5 years after repository closure, respectively, as can be seen in Figure 7. The time at which the amount of H_2 in the repository reaches a maximum (Figure 4) corresponds to the time at which the relatively rapidly corroding C-steel is consumed. The production by H_2 by the corrosion of passivated C-steel, the passive alloys and by Zr is slower than that of C-Steel, and as a result, the H_2 partial pressure in the repository decreases. As shown in Figure 4, the inventory of H_2 drops to zero after approximately 8,000 years and the rate of methanogenesis becomes limited by the rate of production of H_2 by the corrosion of these passive materials.

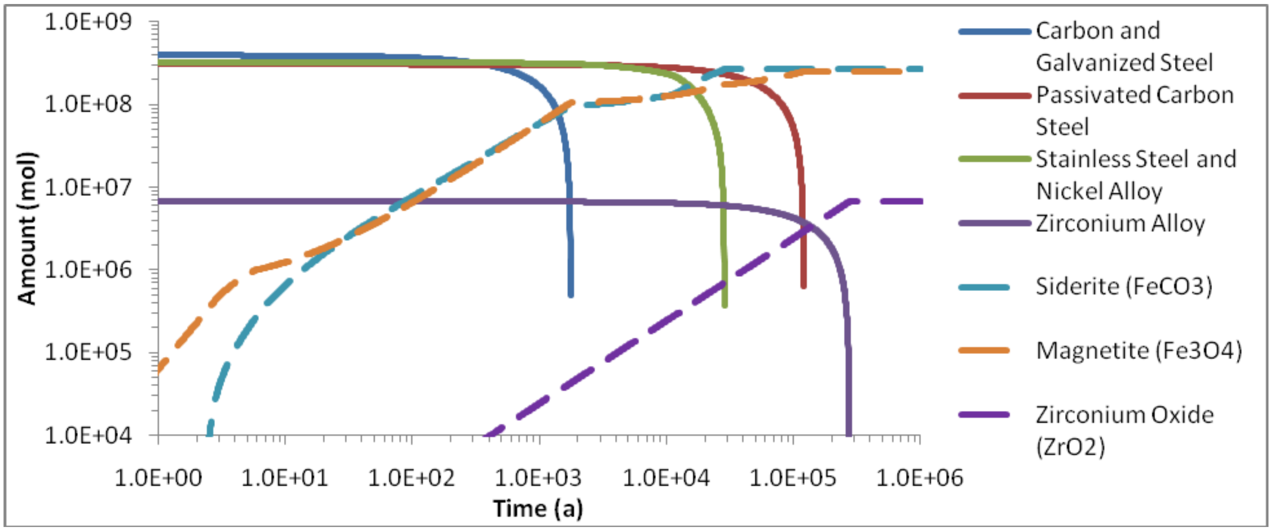

Figure 7: Amounts of Metallic Waste and Corrosion Products

The various corrosion products are given in Figure 7. Approximately 20% of the iron in the metallic waste ends up as siderite ($FeCO_3$) produced through enhanced carbon dioxide corrosion, with most ending up as magnetite (Fe_3O_4). Any "FeOOH" is produced through corrosion in the aerobic degradation stage and is rapidly consumed under anaerobic conditions via Equation (20) of Section 3.1, such that it is completely consumed by the end of the nitrate reduction stage. It then plays no further part in gas evolution.

6. Simplified gas generation model

The standalone GGM testing illustrated in Section 5 has identified four key mechanisms for the generation of gas in the DGR: microbial degradation of organic waste, methanogenesis, corrosion of metallic wastes, and CO_2 enhanced corrosion of metallic wastes.

In order to verify this conclusion, GGM was rerun with the following simplifications:

(1) The initial amounts of terminal electron acceptors (oxygen, nitrate, ferric ion, manganese, and sulphate) were set to zero.

2) Biomass reactions were neglected, including the growth of biomass, recycling and formation of recalcitrant dead biomass. It is assumed that there is enough biomass to support the degradation and gas generation reactions.

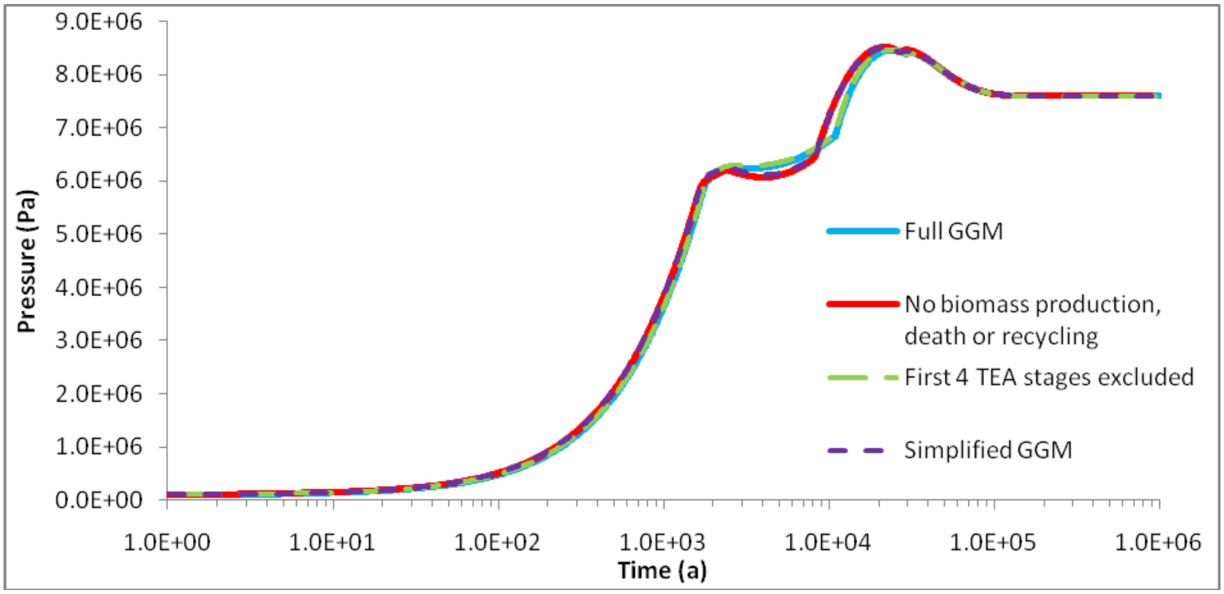

Figure 8: Comparison of Peak Gas pressure in the DGR for Full and Simplified GGM

The results in Figure 8 show that eliminating these reactions had very little effect on the overall response, as expected.

7. Conclusion

Gas generation is one of the key factors in the postclosure safety of OPG's DGR for L&ILW. The GGM model encompasses various microbial and corrosion processes that lead to the generation and consumption of gases in the repository.

Using the standalone GGM, the dominant gas in the repository at long-times was shown to be methane. Four key mechanisms for the generation of gas and the consumption of water in the DGR have been identified:

1. Microbial degradation of organic waste,
2. Methanogenesis,
3. Corrosion of metallic wastes, and
4. CO_2 enhanced corrosion of metallic wastes.

8. References

[1] Calder, N., Avis, J., Humphreys, P., King, F., Suckling, P., Walsh, R., 2009. Postclosure Safety assessment (V1): Gas Modelling. NWMO DGR-TR-2009-07. Toronto, Canada. (http://www.nwmo.ca/dgrpostclosuresafetyassessmentreports)

[2] Little, R., Avis, J., Calder, N., Garisto, N., Humphreys, P., King, F., Limer, L., Metcalfe, R., Penfold, J., Rees, J., Savage, D., Suckling, P., Towler, G., Walke, R., Walsh, R., 2009. Postclosure Safety Assessment (V1) Report. NWMO DGR-TR-2009-01. Toronto, Canada. (http://www.nwmo.ca/dgrpostclosuresafetyassessmentreports)

[3] Suckling, P., Calder, N., Humphreys, P., King, F., Leung, H., 2009. The Development and Use of T2GGM: A Gas Modelling Code for the Postclosure Safety Assessment for OPG's Proposed L&ILW Deep Geologic Repository, Canada. In ICEM/2009 (Liverpool, United Kingdom) paper no. 16291.

[4] Pedersen, K., 1993. The Deep Subterranean Biosphere. Earth-Science Reviews, 34, 243-260.

[5] Grant, W.D., Holtom, G.J., Rosevear, A., Widdowson, D., 1997. A Review of Environmental Microbiology Relevant to the Disposal of Radioactive Waste in a Deep Underground Repository. UK Nirex Report NSS R239. Harwell, UK.

[6] Cohen, S. 2006. Preliminary review of the degradation of cellulosic, plastic, and rubber materials in the Waste Isolation Pilot Plant, and possible effects on magnesium oxide safety factor calculations. Contract Number EP-D-05-002. Work Assignment No. 2-09.

[7] Rittmann, B. E. and McCarty, P. L. 2001. Environmental Biotechnology: Principles and Applications. McGraw –Hill Higher Education.

[8] Hedderich, R., Whitman, W.B., 2006. Physiology and Biochemistry of the Methane-Producing Archaea. In M. Dworkin (ed.), The Prokaryotes: a handbook on the biology of bacteria Volume 2 (p. 1050-1079). New York: Springer.

[9] Thauer, R.K., 1998. Biochemistroy of Methanogenesis: a Tribute to Marjory Stephenson. Microbiology, 144, 2377-2406.

[10] Wang, Y. and Francis, A. J. 2005. Evaluation of Microbial Activity for Long-Term Performance Assessments of Deep Geologic Nuclear Waste Repositories. J. Nucl. Radiochem. Sci., Vol 6, No. 1, pp 43-50.

[11] de Waard, C., Milliams, D., 1975. Carbonic Acid Corrosion of Steel. Corrosion, 31, 177-181.